



1 **Impacts of compound extreme weather events on ozone in the present and future**

2

3 Junxi Zhang¹, Yang Gao^{2*}, Kun Luo¹, L. Ruby Leung^{3*}, Yang Zhang⁴, Kai Wang⁴ and
4 Jianren Fan¹

5

6 ¹State Key Laboratory of Clean Energy, Department of Energy Engineering, Zhejiang
7 University, Hangzhou, Zhejiang, 310027, China

8 ²Key Laboratory of Marine Environment and Ecology, Ministry of Education of
9 China, Ocean University of China, Qingdao, Shandong, 266100, China

10 ³Atmospheric Sciences and Global Change Division, Pacific Northwest National
11 Laboratory, Richland, Washington, 99354, USA

12 ⁴Department of Marine, Earth, and Atmospheric Sciences, North Carolina State
13 University, Raleigh, NC, 27695, USA

14

15 *Correspondence to: Dr. Yang Gao (yanggao@ouc.edu.cn)

16 Dr. L. Ruby Leung (Ruby.Leung@pnnl.gov)

17

18

19

20

21

22

23

24

25

26

27

28

29

30

31

32

33

34

35

36

37

38 **Abstract**

39

40 The Weather Research and Forecasting model with Chemistry (WRF/Chem) was
41 used to study the effect of extreme weather events on ozone in US for historical (2001-
42 2010) and future (2046-2055) periods under RCP 8.5 scenario. During extreme weather
43 events, including heat waves, atmospheric stagnation, and their compound events,
44 ozone concentration is much higher compared to non-extreme events period. A striking
45 enhancement of effect during compound events is revealed when heat wave and
46 stagnation occur simultaneously and both high temperature and low wind speed
47 promote the production of high ozone concentrations. In regions with high emissions,
48 compound extreme events can shift the high-end tails of the probability density
49 functions (PDFs) of ozone to even higher values to generate extreme ozone episodes.
50 In regions with low emissions, extreme events can still increase high ozone frequency
51 but the high-end tails of the PDFs are constrained by the low emissions. Despite large
52 anthropogenic emission reduction projected for the future, compound events increase
53 ozone more than the single events by 10% to 13%, comparable to the present, and high
54 ozone episodes are not eliminated. Using the CMIP5 multi-model ensemble, the
55 frequency of compound events is found to increase more dominantly compared to the
56 increased frequency of single events in the future over the US, Europe, and China. High
57 ozone episodes will likely continue in the future due to increases in both frequency and
58 intensity of extreme events, despite reductions in anthropogenic emissions of its
59 precursors. However, the latter could reduce or eliminate extreme ozone episodes, so
60 improving projections of compound events and their impacts on extreme ozone may
61 better constrain future projections of extreme ozone episodes that have detrimental
62 effects on human health.

63

64 Key words: WRF/Chem, heat waves, stagnation, compound event, high surface ozone

65

66



67

68 **1. Introduction**

69

70 Tropospheric ozone is a secondary air pollutant resulting from complicated
71 photochemical reactions in the presence of its precursors such as volatile organic
72 compounds, NO_x, CO, and CH₄. During the past decades, ozone pollution has been of
73 increasing concern to the public because excessive ozone may have an adverse effect
74 on human health such as increased risk of death (Filleul et al. 2006; Weschler 2006;
75 Gryparis et al. 2004). Ozone also has important effects on agriculture, constructions,
76 and ecology (Sharma et al. 2017; Agrawal et al. 2003). Moreover, as a greenhouse gas,
77 increasing concentrations of ozone may amplify global warming. Thus, it is important
78 to understand factors that govern ozone and its changes in a perturbed environment.

79 Ozone formation is particularly active when favorable meteorological conditions
80 coincide with the presence of precursor emissions (Fiore et al. 2015; Jacob and Winner
81 2009). Meteorological factors that are closely related to ozone formation include daily
82 maximum temperature (Otero et al. 2016), wind speed, cloud cover (Souri et al. 2016;
83 Flynn et al. 2010), etc. Using dynamical downscaling to develop high resolution climate
84 scenarios, Gao et al. (2013) found significant ozone increase in the US during heat wave
85 events, with regional mean maximum daily 8 h average (MDA8) O₃ increases roughly
86 by 0.3 ppbv to 2.0 ppbv compared with non-heat wave period under RCP 8.5. Based on
87 observed data in the US from 2001-2010, Hou and Wu (2016) found significant ozone
88 increase during heat waves in particular for high ozone concentration (i.e., 95th
89 percentile ozone increased by 25%) and PM_{2.5} increase during atmospheric stagnation
90 (i.e., 95th percentile ozone increased by 65%). Both heat waves (Gao et al. 2012;
91 Sillmann et al. 2013; Meehl and Tebaldi 2004) and atmospheric stagnation (Horton et
92 al. 2014) have been projected to increase substantially in the future, suggesting
93 significant impacts on ozone and PM_{2.5} in the future.

94 Going beyond traditional study of single extreme weather events and their impacts,



95 compound effect of extreme events has been explored in recent studies (Zscheischler
96 and Seneviratne 2017). Compound effect can be defined using different criteria
97 including: 1) two or more extreme events occurring simultaneously or successively; 2)
98 combinations of extreme events potentially reinforcing each other; 3) two or more
99 events combined to become an extreme event even though the events themselves are
100 not extreme (Leonard et al. 2014; Seneviratne et al. 2012). The compound effect of
101 more than one extreme weather event has been shown to potentially have a higher
102 impact than a single extreme weather event alone. For example, Zscheischler et al.
103 (2014) concluded that compound effect could be higher than simple additive effect. As
104 an example, they found that the compound effect of heat waves and drought on the
105 global carbon cycle exceeds the additive effect of the individual events. For ozone, heat
106 waves and atmospheric stagnation are two key environmental factors that may lead to
107 compound effect, as high surface temperature under atmospheric stagnation with low
108 wind speed, clear sky, and reduced precipitation and soil moisture may escalate into a
109 heat wave. This motivates the present study to investigate the compound effect of
110 simultaneous occurrence of heat waves and atmospheric stagnation on ozone pollution.

111 Model output from the Coupled Model Intercomparison Project phase 5 (CMIP5;
112 Taylor et al. (2012)) has been widely used to investigate climate change and its impacts.
113 Using a multi-model ensemble such as CMIP5 is particularly important for studying
114 high-impact and low-probability extreme events to yield more robust analyses
115 (Sillmann et al. 2013; Diffenbaugh and Giorgi 2012; Kharin et al. 2013). However, air
116 quality is significantly influenced by regional processes such as cloudiness and
117 mesoscale circulation as well as local emissions. With high spatial and temporal
118 resolutions and more detailed representations of chemical reactions and emission
119 inventory (Gao et al. 2013), regional climate and chemistry models are useful tools that
120 have been widely adopted to study air quality and impact of climate change on air
121 quality (Gao et al. 2013; 2012; Leung and Gustafson 2005; Qian et al. 2010; Yahya et
122 al. 2017a; 2017b). This study combines analysis of regional online-coupled



123 meteorology-chemistry simulations and analysis of the CMIP5 multi-model ensemble
124 to investigate the impact of extreme weather events on ozone concentration in the
125 present and future climate.

126 In what follows, we first investigate the ability of the regional climate-chemistry
127 model in reproducing the observed extreme weather events and ozone concentration in
128 the US. Following the evaluation, the impact of single and compound extreme weather
129 events on ozone concentration at present and future is examined. Lastly, future changes
130 of extreme weather events are discussed in the broader context of the multi-model
131 CMIP5 ensemble.

132

133 **2. Model description and configuration**

134

135 In this study, a modified version of WRF/Chem v3.6.1 (Yahya et al. 2016) was
136 adopted for regional simulations. The detailed modification has been described in
137 Yahya et al. (2016), but the main new features include the extended Carbon Bond 2005
138 (CB05) of Yarwood et al. (2005) gas-phase mechanism with chlorine chemistry of
139 Sarwar and Bhave (2007). The anthropogenic emissions used in WRF/Chem were
140 based on the emissions in RCP8.5 (Moss et al. 2010; van Vuuren et al. 2011) and
141 detailed information of processing the RCP 8.5 emission to model-ready format is
142 available in Yahya et al. (2017b). Biogenic emissions were calculated online in
143 WRF/Chem depending on the meteorology at present or future using the Model of
144 Emissions of Gases and Aerosols from Nature version 2 (Guenther et al. 2006). The
145 meteorological and chemical initial and boundary conditions for WRF/Chem were
146 downscaled from simulations provided by the modified CESM/CAM version 5.3
147 (referred to as CESM_NCSU) (Gantt et al. 2014; He and Zhang 2014; 2017; Glotfelty
148 and Zhang 2016), and the downscaling method has been documented in detail by Yahya
149 et al. (2017b). Two simulation periods using WRF/Chem were selected in this study: a
150 historical period (2001-2010) and a future period (2046-2055), and simulations were



151 performed over the contiguous US (Fig. 1), with a horizontal grid spacing of 36 km and
 152 34 vertical layers from surface to 100 hPa. The simulations for the historical period
 153 have been comprehensively evaluated against surface and satellite observations in
 154 Yahya et al. (2017a) and the projected changes in climate, air quality, and their
 155 interactions for the future period have been analyzed in Yahya et al. (2017b). However,
 156 those results have not been previously evaluated for climate extremes and their impacts
 157 on surface O₃, which is the focus of this work.

158 In addition to the regional model results, output from the CMIP5 ([https://esgf-](https://esgf-node.llnl.gov/search/cmip5/)
 159 [node.llnl.gov/search/cmip5/](https://esgf-node.llnl.gov/search/cmip5/)) multi-model ensemble was used in this study to elucidate
 160 the impact of climate change on compound extreme weather events. A total of 20
 161 CMIP5 models were selected in this study, and the list of models is shown in Table 1.
 162 Variables used in this study mainly include daily maximum near-surface air temperature,
 163 daily precipitation, daily mean near-surface wind speed and daily mean 500 hPa wind
 164 speed, and the data were interpolated to a spatial resolution of 2° × 2°. Three periods
 165 were selected with two periods that overlap in part with that of the regional simulations
 166 (1991-2010 as historical period and 2041-2060 in RCP 8.5), and an additional period
 167 extending to the end of this century (2081-2100).

168
 169
 170

Table 1 A list of the CMIP5 models used in this study

Model	Institution	Resolution (Lon×Lat)	Reference
1. ACCESS1.0	Commonwealth Scientific and Industrial Research Organization (CSIRO), Australia and Bureau of Meteorology (BOM), Australia	1.875×1.25	Bi et al. (2013)
2. ACCESS1.3		1.875×1.25	Dix et al. (2013)
3. BCC-CSM1.1	Beijing Climate Center, China Meteorological Administration	2.81×2.77	Xin et al. (2012)
4. CanESM2	Canadian Centre for Climate Modeling and Analysis, Canada	2.81×2.79	Arora et al. (2011)
5. CMCC-CM	Euro-Mediterraneo sui Cambiamenti Climatici, Italy	0.75×0.75	Scoccimarro et al. (2011)
6. CMCC-CMS		1.875×1.86	Weare et al.



			(2012)
7. CSIRO_Mk3.6.0	Commonwealth Scientific and Industrial Research Organization (CSIRO), Australia	1.875×1.86	Rotstayn et al. (2010)
8. GFDL-ESM2M	NOAA Geophysical Fluid Dynamics Laboratory, USA	2.5×2.0	Donner et al. (2011)
9. GFDL-ESM2G		2.5×2.0	
10. HadGEM2_CC	Met Office Hadley Centre, UK	1.875×1.25	Jones et al. (2011)
11. INM-CM4	Institute for Numerical Mathematics, Russia	2.0×1.5	Volodin et al. (2010)
12. IPSL-CM5A-LR	Institut Pierre-Simon Laplace, France	3.75×1.875	Dufresne et al. (2013)
13. IPSL-CM5A-MR		2.5×1.25	
14. IPSL-CM5B-LR		3.75×1.875	
15. MIROC-ESM	Atmosphere and Ocean Research Institute (The University of Tokyo), National Institute for Environmental Studies and Japan Agency for Marine-Earth Science and Technology	2.81×1.77	Watanabe et al. (2010)
16. MIROC-ESM-CHEM		2.81×1.77	
17. MIROC5		1.41×1.39	
18. MPI-ESM-LR	Max Planck Institute for Meteorology, Germany	1.875×1.85	Zanchettin et al. (2013)
19. MPI-ESM-MR		1.875×1.85	
20. MRI-CGCM3	Meteorological Research Institute, Japan	1.125×1.125	Yukimoto et al. (2012)

171

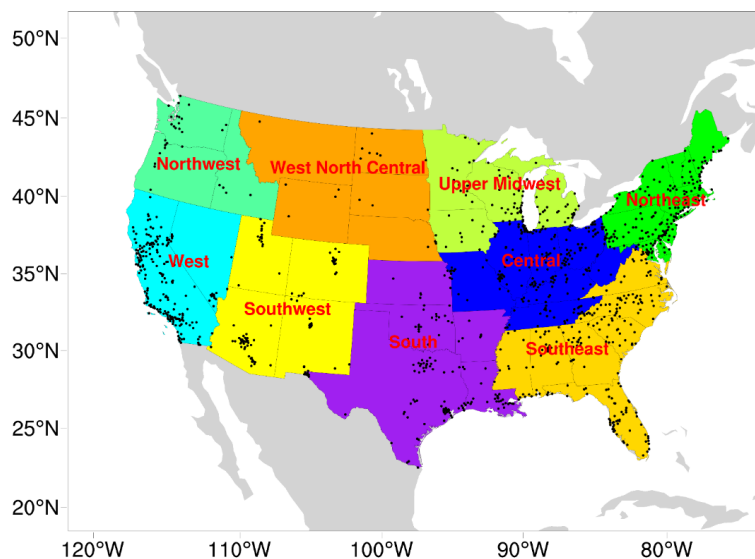
172 3. Evaluation of meteorology and ozone

173

174 The Air Quality System (AQS) dataset (downloaded from
 175 <https://www.epa.gov/aqs>) was used in this study to comprehensively evaluate how well
 176 the WRF/Chem model performs in simulating ozone concentrations, particularly high
 177 ozone concentrations that are more strongly related to extreme weather events. The
 178 locations of observation stations in AQS are shown in Fig. 1 and overlaid on nine
 179 climate regions in the US. For evaluation of simulated extreme weather events, the
 180 NCEP North American Regional Reanalysis (Mesinger et al. 2005) dataset was used.



181



182

183 Fig. 1. The WRF/Chem simulation domain and climate regions in the US. The red
184 points (~ 1200) represent the observation stations of O_3 in AQS.

185

186 3.1 Evaluation of extreme weather events

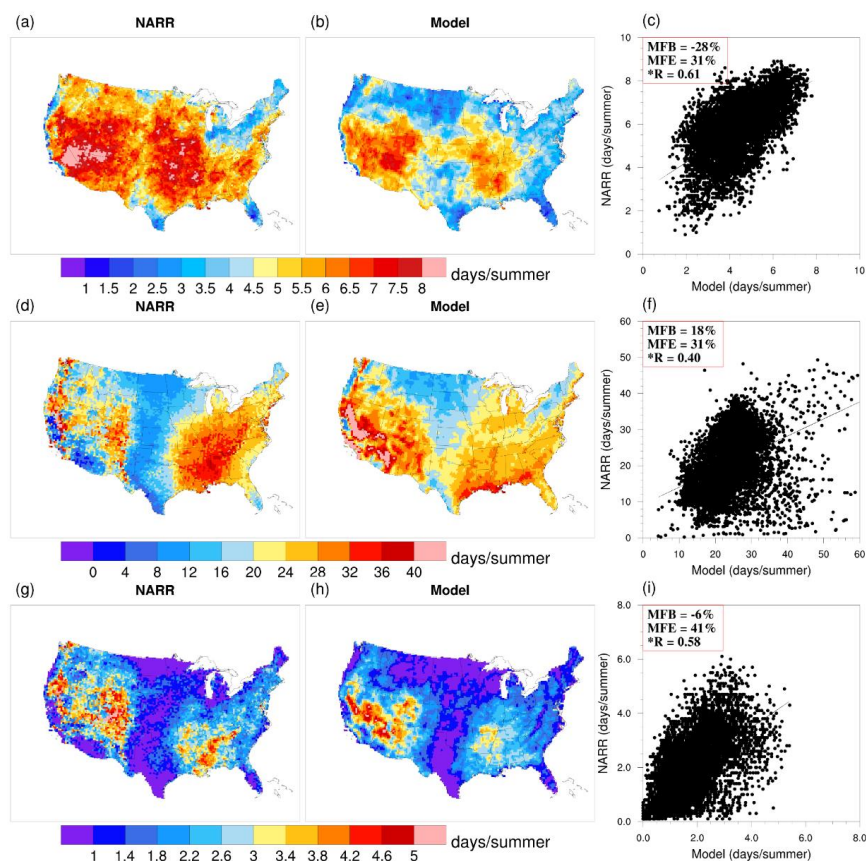
187

188 Two types of extreme weather events including heat waves and atmospheric
189 stagnation, as well as their compound events were investigated considering their close
190 relationship with ozone pollution. A heat wave is defined to occur when daily maximum
191 2-meter air temperature exceeds a certain threshold continuously for three days or more.
192 The threshold is set as the 97.5th percentile of the historical period (2001-2010 for
193 WRF/Chem and 1991-2010 for CMIP5 in this study) and is location dependent to take
194 into account the wide-ranging characteristics of different regions (Gao et al. 2012;
195 Meehl and Tebaldi 2004). An atmospheric stagnation day is defined to occur when daily
196 mean 10-m wind speed, daily mean 500 hPa wind speed, and daily total precipitation
197 are less than 20% of the climatological mean condition (2001-2010 for WRF/Chem in
198 this study) (Horton et al. 2014; Hou and Wu 2016). A compound event occurs when
199 both heat wave and atmospheric stagnation occur simultaneously on the same day. For
200 each grid, the same threshold determined for the present period is used for the future



201 period to evaluate the future changes.

202 To evaluate the ability of the regional model in reproducing the extreme weather
203 events, Fig. 2 shows the distribution of mean number of summer heat wave days,
204 atmospheric stagnation days, and compound event days corresponding to coincidental
205 heat wave and atmospheric stagnation during 2001-2010. Observations based on the
206 NARR dataset and the model results are shown, along with scatterplots comparing the
207 observations and simulations at each NARR grid point over land. Statistical metrics,
208 including mean fractional bias (MFB), mean fractional error (MFE) and correlation
209 coefficient (R), based on the formulae (A2), (A3) and (A6) in the appendix, are shown
210 in the scatterplots.



211
212 Fig. 2. Distribution of mean number of extreme weather days in summer of 2001-
213 2010 from observations (NARR; left panels) and model simulations (middle panels)



214 and scatterplots comparing them at each NARR grid point over land (right panels) for
215 heat wave days (Figs. 2a,b,c), atmospheric stagnation days (Figs. 2d,e,f) and
216 compound event days (Figs. 2g,h,i). The numbers located on the top left of the
217 scatterplots (Fig. 2c,f,i) indicate the statistical metrics including mean fractional bias
218 (MFB), mean fractional error (MFE) and correlation coefficient (R). A r-test ($\alpha=0.05$)
219 for the linear correlation coefficient was performed and *R indicates statistical
220 significance at 95% confidence level.

221

222 The spatial distributions of both heat waves and atmospheric stagnation are
223 generally consistent between NARR and WRF/Chem (top and middle rows). For
224 example, for heat waves (Figs. 2a,b), the model captures the high frequency of
225 occurrence in the western US and eastern central US albeit widespread
226 underestimations particularly in the northern US and the central Great Plains. For
227 atmospheric stagnation (Figs. 2d,e), the observed dipole feature of high frequency of
228 occurrence in the western and eastern US, separated by the central Great Plains, is well
229 reproduced by the model but biases in the magnitude are noticeable. To quantitatively
230 evaluate the simulations, the WRF/Chem model results were bilinearly interpolated to
231 the NARR grid suggested by USEPA (2007), and scatterplots were drawn to show the
232 results for all the NARR grid points (Figs. 2c,f). No benchmark is available regarding
233 the statistical metrics for extreme weather events but we adopt the benchmarks widely
234 used in air quality studies. For example, USEPA (2007) suggested 15%/35%
235 (MFB/MFE) for O₃ and 50%/75% (MFB/MFE) for PM_{2.5} species. From this
236 perspective, the MFB and MFE for either heat waves or atmospheric stagnation are
237 within or close to the benchmarks for O₃, and well within the benchmarks for PM_{2.5}
238 species. Moreover, the model results are correlated with NARR, with R equals to 0.61
239 and 0.40, respectively, for heat waves and atmospheric stagnation and statistically
240 significant at 95% confidence level.

241 The western US receives most of its precipitation in the cold season when the
242 North Pacific jet stream steers storm tracks across the region. During summer, the North
243 Pacific subtropical high pressure center expands and exerts a stronger influence on the
244 western US, increasing the frequency of atmospheric stagnation. Combining the low



245 wind speed and low probability of precipitation during stagnation with low antecedent
246 soil moisture condition generally prevalent during summer, heat waves can develop to
247 create a maximum center of combined extreme events beyond the coastal mountain
248 ranges of the western US. The eastern central US is prone to heat wave and stagnation
249 as a result of the upper level ridge that develops during summer in that region. These
250 climatic conditions give rise to the dipole patterns of maximum heat wave and
251 stagnation in the western and eastern central US. The dipole pattern becomes more
252 obvious and magnified for the compound events because stagnation can promote the
253 development of heat waves, as discussed earlier. For the compound events, the
254 simulation performs well and even better than the metrics of atmospheric stagnation
255 events. The high values in western and southeastern US, as well as the low values in
256 the central and upper Midwestern US are reasonably captured by the model, with
257 statistically significant correlation ($R=0.58$).

258 Thus, WRF/Chem in general well reproduced the spatial patterns and frequency
259 of the extreme weather events including heat waves, atmospheric stagnation, and their
260 compound events. Although atmospheric stagnation occurs more than 20 days during
261 the summer in large areas over the western and eastern US, heat waves do not occur for
262 more than 10 days generally, so the compound events of heat waves and stagnation are
263 rather rare and occur on average for no more than 5 days during summer over the US.
264 In the next section, ozone concentrations during these extreme weather events are
265 analyzed.

266

267 **3.2 Evaluation of ozone concentrations during extreme weather events**

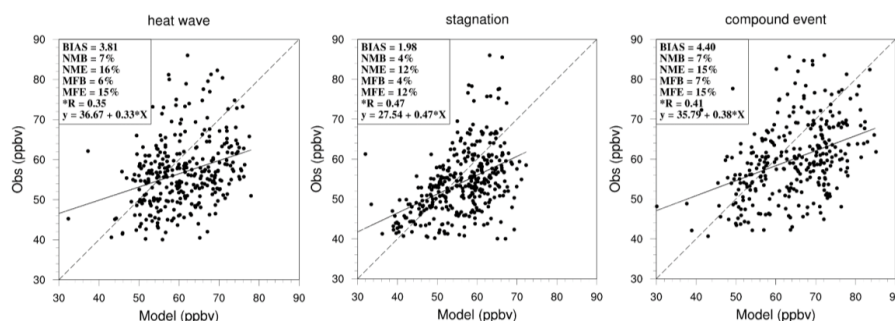
268

269 Maximum daily 8-hr (MDA8) ozone is an important variable considering its close
270 relationship with human health (USEPA 2007) so we focus on the evaluation of MDA8
271 O_3 during summertime. From the perspective of public health, USEPA (2007)
272 recommended attention to ozone values higher than 40 ppbv because the human impact
273 of ozone is small for low ozone concentration. Thus, we compare the mean ozone



274 concentrations during summer of 2001-2010 between observed data (AQS) and model
275 results for the following three conditions in Fig. 3: 1) days with heat waves, but no
276 atmospheric stagnation; 2) days with atmospheric stagnation but no heat waves; 3) days
277 with compound events (both heat wave and atmospheric stagnation) occurring. Thus
278 the first two conditions identify single extreme events and the third condition identifies
279 compound extreme events. We compare observed ozone concentration greater than or
280 equal to 40 ppbv and the simulated ozone concentration corresponding to the same
281 locations of the observations.

282 As depicted in Fig. 3, WRF/Chem reasonably reproduced the observed ozone
283 concentrations during the extreme weather events, showing statistically significant
284 correlations with the observed AQS data. Moreover, if the benchmark (15%/35% for
285 MFB/MFE and 10%/20% for NMB/NME) suggested by USEPA (2007) is used as a
286 reference, all the statistical metrics based on evaluation against ozone higher than 40
287 ppbv in observations are within or much smaller than the benchmarks, illustrating
288 promising ability of WRF/Chem in simulating the ozone concentrations during heat
289 waves, stagnation, and their compound events. Even if all ozone values including values
290 below 40 ppbv are considered, the four metrics (MFB/MFE and NMB/NME) are mostly
291 within the benchmarks and the correlation coefficients between model and observation
292 are only slightly reduced by 0.04, 0.11, and 0.1 for the three types of extreme weather
293 events, respectively, and all values are still statistically significant. However, the
294 general low biases of the simulations are obvious from the regression lines. Ozone
295 concentrations during compound extreme events are clearly shifted to higher values
296 relative to ozone concentrations during single extreme events.



297

298 Fig. 3. Ozone concentration comparison between observations (AQS) and WRF/Chem
299 simulations during heat waves (left), atmospheric stagnation (middle), and
300 heat wave and atmospheric stagnation events (right). Metrics shown inside each figure
301 were from formula (A1) to (A6) in the Appendix. An *r*-test ($\alpha=0.05$) is performed to
302 test the statistical significance and **R* indicates statistical significance at 95%
303 confidence level. The solid line is the linear regression line, and the dashed line is a
304 one-to-one reference line.

305

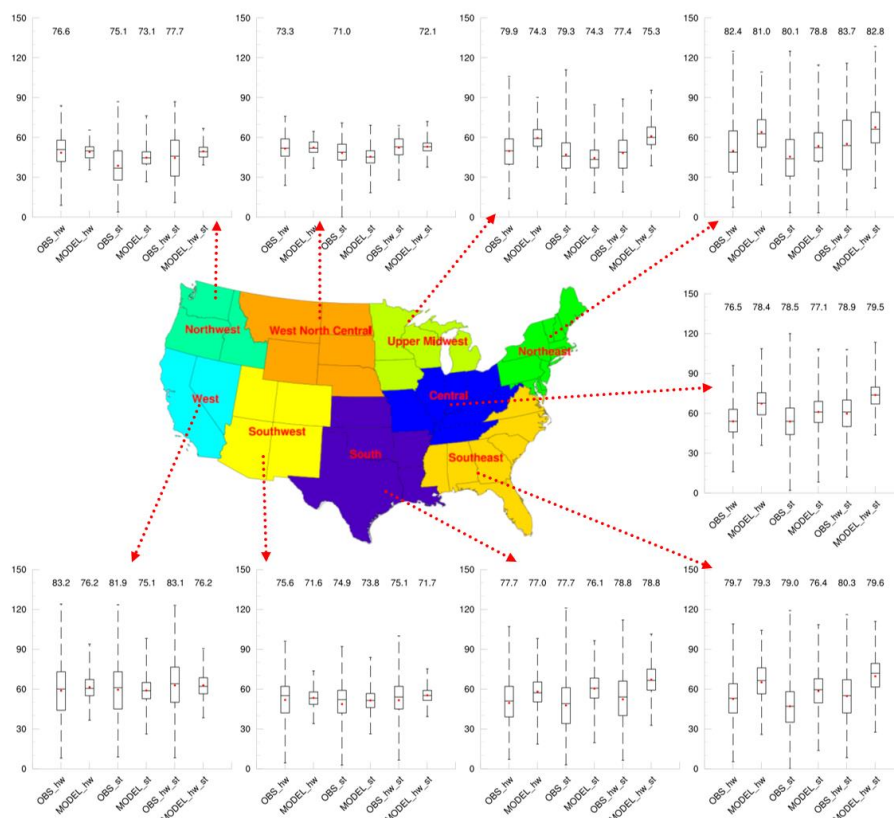
306 To delve into the spatial heterogeneity, ozone concentrations from model and
307 observations for the three types of extreme weather events are shown using box-and-
308 whisker plots in Fig. 4. Considering the detrimental effect on human health when
309 MDA8 ozone concentration exceeds 70 ppbv by National Ambient Air Quality
310 Standards (NAAQS), we evaluate the WRF/Chem simulated ozone concentrations
311 above this particular threshold. We calculated the mean values of MDA8 ozone
312 concentration exceeding 70 ppbv for each type of extreme weather events, and the mean
313 values are marked at the top of each panel in Fig. 4.

314

315 The box-and-whisker plots show some unique features in the observations. For
316 example, the mean ozone (red dot) concentrations tend to be slightly higher when heat
317 waves and stagnation occur at the same time, while the mean values are relatively lower
318 during atmospheric stagnation than during heat waves. These are consistent with Fig. 3
319 when values are plotted regardless of the regions. This feature was well captured by the
320 model, in particular over regions in the eastern US, such as Northeast and Southeast.
321 Regarding high ozone concentrations (i.e., values higher than 70 ppbv), the model has
322 considerable skill in the eastern US with major anthropogenic emissions. The mean bias
could be as small as 0.4 ppbv (over the Southeast during heat waves), and mostly within



323 1 ppbv. However, for some regions, i.e., West and Southwest, negative biases could
324 reach a few ppbv; the negative biases in many regions are likely linked to an
325 underestimation of heat wave intensity, which is reflected in the underestimation of heat
326 wave days as shown in section 3.1. Other possible reasons for the negative biases in
327 surface O₃ include uncertainties in precursor emissions, boundary conditions, as well
328 as overpredictions in precipitation, as reported in Yahya et al. (2017a).
329



330
331 Fig. 4. MDA8 ozone concentration comparisons during the summer of 2001-2010 in
332 nine climate regions, with box-and-whisker plots showing the minimum, maximum
333 (line end-points), 25th percentile, 75th percentile (boxes), medians (black lines) and
334 average (red point) of mean MDA8 ozone from observation (with prefix OBS_) and
335 model (with prefix MODEL_) during heat waves (with suffix hw), atmospheric
336 stagnation (with suffix st) and compound events of both heat wave and atmospheric
337 stagnation (with suffix of hw_st). The numbers at the top of each panel indicate the
338 average values of MDA8 ozone concentration above the standard (70ppbv).



339

340 **4. Impacts of extreme events and climate change on ozone**

341 **concentrations**

342

343 **4.1 Impacts of single and compound extreme events on ozone**

344 **concentrations**

345

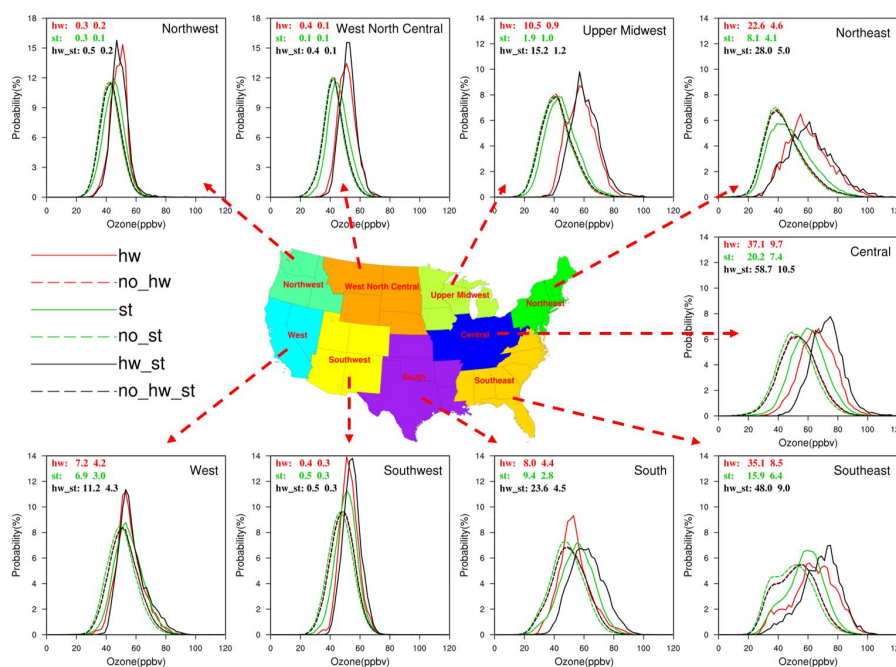
346 To investigate the impacts of the extreme weather events on ozone concentrations,
347 we composited the MDA8 ozone concentrations from WRF/Chem for the three types
348 of extreme weather events and to the corresponding non-extreme event periods in
349 summer of 2001-2010 using probability density functions (PDFs) shown in Fig. 5.

350 By comparing the solid lines (extreme event period) and dashed lines (non-
351 extreme event period) in Fig. 5, all extreme weather events have positive impacts on
352 ozone particularly at the high-end tail of the distributions. The difference between
353 ozone concentrations with and without extreme events is statistically significant in all
354 regions at the 95% confidence level. For regions with mean ozone values exceeding 70
355 ppbv (numbers shown in Fig. 5), much larger differences are noticeable between the
356 PDFs of extreme and non-extreme periods, with extreme events notably shifting both
357 the low-end and high-end tails towards higher values. These regions include Northeast,
358 Central, South, and West. Conversely, regions such as Northwest, West North Central
359 and Southwest show negligible differences between the PDFs. The spatial
360 heterogeneity is closely related to the spatial distribution of emissions in the US, i.e.,
361 regions with larger increase of ozone concentration particularly near the high-end tail
362 (i.e., Northeast, Southeast, Central, Upper Midwest, South and West) due to extreme
363 weather events are also areas with higher anthropogenic emissions in the US (see also
364 Fig. 3 in Gao et al. (2013)). Thus, stronger photochemical reactions in those regions
365 may enhance the effect of extreme weather events on ozone formation.

366 Now comparing the effects of different types of extreme weather events on ozone



367 concentrations (solid lines of different colors in Fig. 5), the effect of heat waves on
 368 ozone formation is generally larger than the effect of atmospheric stagnation, whereas
 369 the compound effect is larger than the effect of either type of single extreme weather
 370 event. This feature displays similar spatial heterogeneity as discussed above, i.e., the
 371 largest impact from the compound effect occurs in the South and Central (about half of
 372 the compound events leading to MDA8 ozone higher than 70 ppbv), followed by
 373 Northeast, South, Upper Midwest and West (11%-28% compound event days resulting
 374 in MDA8 O₃ of 70 ppbv or higher) and negligible increase from the compound events
 375 for other regions (Northwest, West North Central and Southwest).
 376

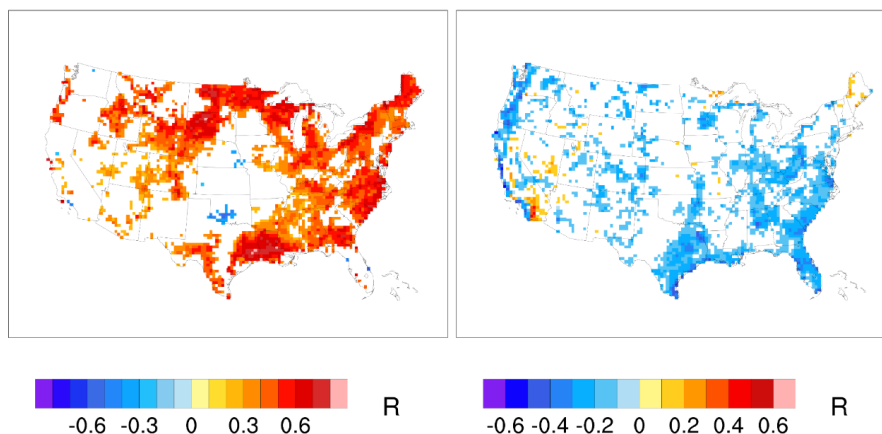


377
 378 Fig. 5. Compositing probability density distributions of MDA8 ozone for three types of
 379 extreme weather events (solid lines) and non-extreme event periods (dashed lines)
 380 during summer of 2001-2010. Each panel includes two numbers on the upper left
 381 showing the probability of MDA8 ozone higher than 70ppbv during extreme weather
 382 events (left) and non-extreme periods (right) for heat waves (hw: red), stagnation (st:
 383 green), and compound extremes events (hw_st: black). Note that all panels except for
 384 the Northwest and West North Central use the same scale for the y-axis
 385

386 Besides the distinguishing impacts extreme events have on ozone relative to non-



387 extreme days, how high the concentration of ozone can reach during extreme events
388 may depend on the intensity of the extreme events and the emissions. Fig. 6 shows the
389 correlations between ozone concentration with the daily maximum 2-meter temperature
390 during heat waves and 10-meter wind speed during atmospheric stagnation events. The
391 correlations between temperature and ozone are positive and statistically significant in
392 areas with high emissions such as Northeast, Central, Upper Midwest, South, and
393 Southeast. For stagnation events, the correlations are statistically significant mainly in
394 South, Southeast, and along the west coast. These correlations between ozone and the
395 intensity of extreme events are consistent with the shift of the high-end tails of the PDFs
396 to higher ozone values, as shown in Fig. 5. In areas with low emissions (e.g., Northwest
397 and West North Central), ozone concentrations are not well correlated with the intensity
398 of extreme events because the production of ozone is limited by the low emissions.
399 Hence only the low-end instead of the high-end tails of the PDFs are shifted to higher
400 values in regions with low emissions, and the PDFs on extreme days are noticeably
401 narrower compared to the PDFs on non-extreme days (Fig. 5). As climate change may
402 increase the frequency as well as the intensity of extreme events, ozone concentrations
403 may be affected, regardless of emissions control in the future.
404



405
406 Fig. 6. Correlation between ozone concentration and (left) daily maximum 2-meter
407 temperature during heat waves and (right) 10-meter wind speed during atmospheric
408 stagnation. Only values that pass the t-test of statistical significance ($\alpha=0.05$) are



409 shown in colors.

410

411 **4.2 Impacts of climate change on ozone concentrations**

412

413 Having investigated the impacts of extreme weather events on ozone
414 concentration, we now focus on how ozone concentrations may change in the future
415 with climate change, changes in biogenic emissions in response to changes in climate,
416 and large anthropogenic emission reductions in the RCP 8.5 scenario. Fig. 7 shows the
417 spatial variations of ozone concentrations composited during extreme weather events
418 at present (top row) and in the future (bottom row). The spatial features displayed in
419 the top row are in agreement with what have been observed from Fig. 5, showing larger
420 impacts of extreme weather events on ozone formation east of the Rockies for both
421 single extreme events and compound events (Figs. 7a,b,c). Similarly large impacts are
422 also found in California, which are obscured in the regional average shown in Fig. 5.
423 Averaged over the US, MDA8 ozone concentrations increase by 22% and 12% during
424 heat waves and stagnation events compared to non-heat wave and non-stagnation days.
425 Compound events have significantly higher impact on ozone compared to the single
426 extreme events, with statistically significant differences of 13% and 16%, respectively,
427 for heat waves and stagnation (Figs. 7d,e). To understand why compound events have
428 larger impacts than single extreme events, Fig. S1 shows that on compound event days,
429 the daily maximum 2-meter temperature is comparable to that during heat waves but
430 6.27°C higher than that during stagnation events, leading to a 16% increase in MDA8
431 O₃ during compound events relative to stagnation events. Similarly, the 10-meter wind
432 speed during compound events is comparable to that during stagnation events but 1.4
433 ms⁻¹ weaker than during heat wave days, leading to a 13% increase in MDA8 O₃ relative
434 to heat wave days.

435 In the future, as anthropogenic emissions are projected to decrease substantially
436 (i.e., Table 2 in Gao et al. (2013)), the mean ozone concentration correspondingly
437 decreases during both single extreme events and compound events compared to the



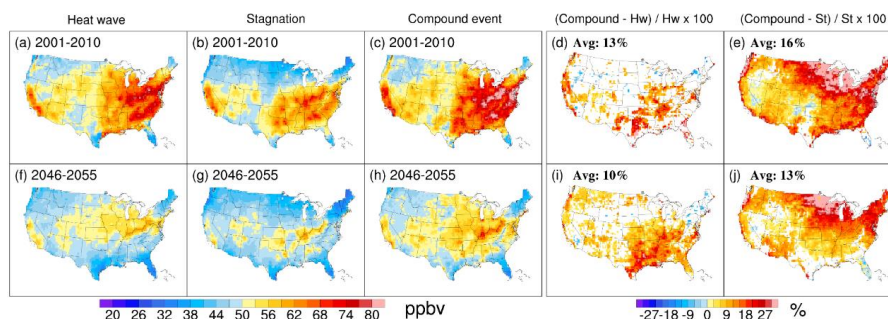
438 present day (i.e., Figs. 7f,g,h vs. Figs. 7a,b,c). However, even with the dramatic
439 anthropogenic emission reduction (i.e., 50% or more reduction in non-methane volatile
440 organic compounds and nitrogen oxides based on Table 2 in Gao et al. (2013)), extreme
441 weather events can still trigger the formation of high ozone concentration (e.g., in
442 central eastern US in Figs. 7f,g,h) to reach or exceed the present-day national standard
443 of 70 ppbv. From Fig. S1, the daily maximum 2-meter temperature is 5.54°C warmer
444 during compound events than stagnation events, leading to a 13% increase in MDA8
445 O₃ during compound events relative to stagnation events. Similarly, the 10-meter wind
446 speed is 1.28 ms⁻¹ weaker during compound events than heat wave events so MDA8 O₃
447 increases by 10% during compound events relative to heat wave events in the future.
448 Hence, compound events increase ozone concentrations by 10% and 13% more than
449 the effect of heat wave only and stagnation only, respectively. These numbers shown in
450 Figs. 7i, j are only 3% lower than those of the present day (Figs. 7d,e).

451 Despite dramatic reduction in anthropogenic emissions in the RCP 8.5 scenario,
452 extreme weather events are still important considerations for air quality and health in
453 the future. This is because both frequency and intensity of extreme events increase in
454 the future, which compensate partly for the effects of reduced emissions. From Fig. S2,
455 heat waves occur on average 13.67 days more and 0.98°C warmer in the future relative
456 to the present, with most of the increase occurring in the western US. There is no
457 increase in the number of stagnation days in the future when averaged over the US (Fig.
458 S2), and the change in wind speed during stagnation is also negligible (Fig. S3).
459 However, the daily maximum 2-meter temperature is 1.42°C warmer during stagnation
460 events in the future compared to the present (Fig. S2). Lastly, compound events occur
461 on average 4.91 days more often, with temperature 1.25°C warmer in the future
462 compared to the present (Fig. S2). Hence the increase in the number of heat waves and
463 the warmer temperature during heat waves as well as stagnation events increase their
464 individual and compound effects on ozone concentrations in the future. These motivate
465 analysis of changes in extreme events in the future using a multi-model ensemble for



466 more robust results.

467



468

469 Fig. 7. Spatial distributions of mean MDA8 ozone concentrations for three types of
470 extreme weather event episodes and the relative difference between compound event
471 and single event during summer in 2001-2010 (top row) and 2046-2055 under RCP 8.5
472 (bottom row). In (d,e,i,j), only values with statistically significant differences (t-test:
473 $\alpha=0.05$) between the compound effect and single event are shown, and the mean
474 differences are labelled on the top left.

475

476 5. Changes of extreme weather events in future by CMIP5

477

478 To provide further insight of future changes in ozone concentration, we analyzed
479 changes in extreme weather events using the multi-model ensemble of CMIP5 data.
480 Using CMIP5 data complements our analysis of the WRF/Chem simulations in two
481 ways. First, CMIP5 model outputs are available for a continuous period through 2100.
482 We analyzed three time periods, each 20 years long, for 1991-2010 as historical period,
483 and 2041-2060 and 2081-2100 in RCP 8.5 as future periods. Extending the analysis
484 period from 10 years for the regional climate simulations to 20 years for CMIP5 allows
485 for a more statistically robust analysis of extreme events. The added period of the late
486 century, 2081-2100, will elucidate how extreme weather events evolve with continuous
487 warming. Second, we extended our analysis using CMIP5 data to the entire northern
488 hemisphere starting from 20°N. The inclusion of other continents such as Europe and
489 China provides useful information for how extreme weather events may change in
490 densely populated regions, with potential impacts on air quality and health.

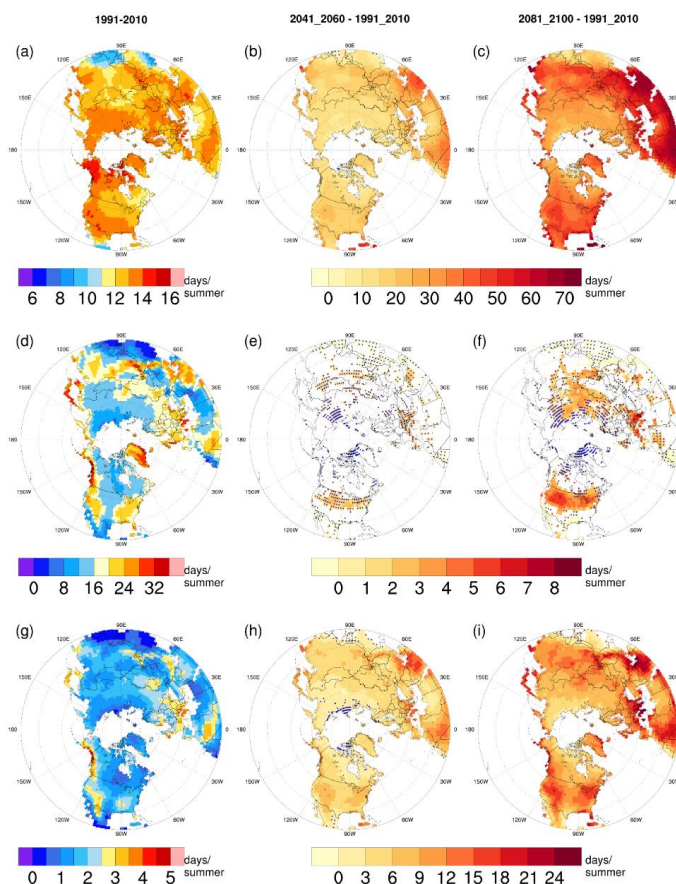


491 The summer mean number of days at present (1991-2010) and changes in future
492 (2041-2060, 2081-2010) for heat waves, atmospheric stagnation, and compound events
493 are shown in Fig. 8. For robust comparisons between future and present climate, both
494 model agreement and significance are considered, as adopted by previous studies (Gao
495 et al. 2014; Seager et al. 2013; Tebaldi et al. 2011). A total of 20 models were selected
496 (listed in Table 1), and values at any grid cell are considered to have agreement if more
497 than 70% of the models agree with the CMIP5 mean on the sign of the change. Once
498 agreement is established, statistical significance is tested over the grid cells, and the
499 values at any grid cell are statistically significant if at least half of the CMIP5 models
500 show statistical significant changes (t-test, $\alpha=0.05$). After the tests, most of the grid
501 cells showing model agreement also passed the statistical significance test; blue dots
502 indicate grid cells with no significant changes of extreme weather events. Three major
503 continents were selected for analysis and the results are summarized in Table 2.

504 As shown in Fig. 8 and Table 2, at present (Figs. 8a,d,g), the mean annual numbers
505 of heat waves, atmospheric stagnation and compound events are 12.9, 16.4 and 1.6,
506 respectively. In the future, there are robust increases of heat wave days worldwide,
507 consistent with previous studies (Sillmann et al. 2013), with a mean increase around
508 200% by the end of this century. The changes in atmospheric stagnation are in general
509 smaller than the changes in heat waves; however, large increases can also be found in
510 some areas such as the western US. This is in contrast with the insignificant change in
511 stagnation days from the WRF/Chem simulation (Fig. S2), demonstrating the
512 importance for using a multi-model ensemble and investigating changes not just in the
513 mid-century but further towards the end of the century when climate change signals
514 become more prominent (Figs. 8e,f). The overall increase in stagnation events is on
515 average 1 day per summer in the future over the northern hemisphere for atmospheric
516 stagnation by the end of this century. Moreover, it is obvious that the compound event
517 shows more dominant increases than stagnation event, with 2 days or less at present on
518 average, but more than 10 days on average in the US, Europe and China. Since we have



519 demonstrated that compound events have larger impact on ozone than single extreme
520 events (Fig. 5), the large increase in compound event days suggests that they will be
521 important considerations for projecting high ozone episodes.
522



523
524 Fig. 8. Spatial distribution of historical (left column) and future changes in the mid-
525 century (second column) and end-of-century (third column) in the number of extreme
526 weather days per summer for heat waves (top row), atmospheric stagnation (middle
527 row) and compound events (bottom row) from CMIP5 over land in the north
528 hemisphere north of 20° N. For the future changes, only grids showing model
529 agreement are shown, with blue dots representing values with no statistical
530 significance.
531

532 As discussed in Section 4, both the frequency and intensity of extreme events have
533 important effects on ozone concentrations. From Fig. S4, the intensity of heat waves



534 is projected to increase with time throughout the 21st century as warming increases.
 535 Both the WRF/Chem and CMIP5 results show larger increase in heat wave intensity
 536 in the western US. During stagnation and compound events, the daily maximum 2-
 537 meter temperature also increases with time. Consistent with WRF/Chem results (Fig.
 538 S3), CMIP5 also shows negligible changes in wind speed during atmospheric
 539 stagnation and compound event, but decrease during heat waves (Fig. S5), further
 540 enhancing the effect on ozone formation.

541

542 Table 2. Average number of days of extreme weather event episodes in summer of 1991-
 543 2010, 2041-2060 and 2081-2100, along with the future increase over the northern
 544 hemisphere (NH) and three regions including the United States (US), Europe, and
 545 China. Statistical significance test was applied using a t-test ($\alpha=0.05$), and values with
 546 no statistical significance are italicized.

547

Areas	Heat wave (days/summer)		
	Hist (1991~2010)	2041~2060 - Hist	2081~2100 - Hist
NH	12.9	15.6	36.5
US	13.3	17.3	39.7
Europe	13.1	16.0	37.8
China	12.3	16.3	39.2
Areas	Stagnation (days/summer)		
	Hist(1991~2010)	2041~2060 - his	2081~2100 - Hist
NH	16.4	<i>0.2</i>	<i>0.9</i>
US	18.0	<i>0.6</i>	<i>1.7</i>
Europe	21.9	<i>0.2</i>	<i>0.9</i>
China	17.4	<i>0.1</i>	<i>0.6</i>
Areas	Compound events (days/summer)		
	Hist (1991~2010)	2041~2060 - Hist	2081~2100 - Hist
NH	1.6	4.1	9.2
US	2.0	5.1	11.3
Europe	1.9	4.9	11.5
China	1.6	4.6	10.5

548

549 6. Conclusions and Discussions

550



551 The region model WRF/Chem version 3.6.1 has been used to downscale
552 simulations from the CESM_NCSU global model. The regional model well reproduced
553 the frequency of extreme weather events, including heat waves, atmospheric stagnation
554 and their compound events, and the ozone concentration during these extreme weather
555 events at present, compared to observations. Through comparison of ozone
556 concentrations during extreme weather events period and non-extreme period, we
557 established statistically significant higher ozone concentrations during the extreme
558 event period. In particular, compound events yield the highest contribution to high
559 ozone formation, followed in general by heat waves and atmospheric stagnation.

560 Compound events have larger impacts on ozone than single events because the
561 temperature during compound events is noticeably higher than that during stagnation-
562 only events and the wind speed during compound events is noticeably weaker than
563 during heat wave-only events. The combination of warmer temperature and weaker
564 winds promote photochemical reactions that produce high ozone episodes. Also
565 importantly, ozone concentrations increase with the intensity of extreme events in
566 regions with high emissions, leading to a shift in the PDFs towards higher ozone values,
567 and increasing the frequency of occurrence of high ozone episodes. In regions with low
568 emissions, extreme events noticeably increase the ozone concentrations at the low-end
569 tails, but the high-end tails are not shifted, leading to narrower PDFs during extreme
570 events relative to non-extreme events.

571 In the future, under the RCP 8.5 scenario, albeit large reductions in anthropogenic
572 emissions projected, extreme weather events can still trigger the formation of higher
573 ozone concentration. The increase in ozone concentrations during extreme events
574 relative to non-extreme events is comparable in the future as in the present. Furthermore,
575 compound events of heat waves and stagnation continue to have larger impacts on
576 ozone concentrations relative to the single weather extreme events. By utilizing a total
577 of 20 CMIP5 models, we found that under climate warming, more frequent extreme
578 weather events are projected to occur in mid- to end of this century. Among the



579 increases by the end of the century, compound events show a dominantly higher
580 fractional increase by a factor of 4-5, compared to the single events, i.e., heat waves (~
581 a factor of 2) or atmospheric stagnation (~ 14%), as shown in Table 2.

582 Since the CMIP5 models do not include detailed atmospheric chemistry, we cannot
583 assess how ozone concentrations may change in the mid-to-late 21st century. The
584 CMIP5 results indicate robust increases in the frequency and intensity of heat waves
585 and frequency of compound events with higher temperature in the future. While
586 reductions of anthropogenic emissions in the RCP 8.5 scenario will likely counter the
587 effects of extreme events on ozone concentrations, the frequency of high ozone
588 concentrations is enhanced by extreme events even in low emission regions (e.g.,
589 Northwest) in the present day (Fig. 5). Hence it is likely that high ozone episodes may
590 still occur in the future due to increases in extreme heat, despite reductions in
591 anthropogenic emissions, with adverse effect to human health.

592 However, similar to how low emissions constrain the high-end tails of the PDFs
593 of ozone from shifting to very high or extreme ozone concentrations even under
594 extreme weather conditions (e.g., Northwest in Fig. 5), reductions in anthropogenic
595 emissions in the future could reduce or eliminate the occurrence of extreme high ozone
596 episodes. Hence controlling anthropogenic emissions may be critical for reducing the
597 impacts of extreme events on extreme air quality episodes and associated human health
598 impacts. This may be especially important in regions like China that have experienced
599 severe air pollution in the recent decades. More attention to improving projections of
600 compound events and evaluating their impacts on ozone may better constrain the
601 projections of extreme air quality episodes and inform strategies to reduce their
602 detrimental effects on human health now and in the future.

603

604 **Appendix**

605

606 **Statistically metrics for evaluating model performance**

607



608 Metrics for model performance evaluation used in this study include BIAS (Mean
 609 Bias), NMB (Normalized Mean Bias, percent), NME (Normal Mean Error, percent),
 610 MFB (Mean Fractional Bias, percent), MFE (Mean Fractional Error percent) and R
 611 (Correlation Coefficient). Calculations of these metrics are shown below in Eqs. (A1)-
 612 (A5), where N is the number of sample size, MODEL and OBS represent the
 613 corresponding value in model simulation and observation (AQS sites or reanalysis data),
 614 respectively. As low OBS values can amplify the metrics, a cutoff of 40 ppbv or 60
 615 ppbv of ozone is suggested in evaluation for ozone. Benchmarks of MFB and MFE for
 616 O₃ are 15% and 35%, and of NMB and NME for O₃ are 10% and 20% (USEPA 2007).

$$617 \quad BIAS = \frac{1}{N} \sum_1^N (Model - Obs) \quad (A1)$$

$$618 \quad NMB = \frac{\sum_1^N (Model - Obs)}{\sum_1^N (Obs)} \times 100\% \quad (A2)$$

$$619 \quad NME = \frac{\sum_1^N |Model - Obs|}{\sum_1^N (Obs)} \times 100\% \quad (A3)$$

$$620 \quad MFB = \frac{2}{N} \sum_1^N \left(\frac{Model - Obs}{Model + Obs} \right) \times 100\% \quad (A4)$$

$$621 \quad MFE = \frac{2}{N} \sum_1^N \left(\frac{|Model - Obs|}{Model + Obs} \right) \times 100\% \quad (A5)$$

$$622 \quad R = \frac{\sum_1^N (Model - \overline{Model})(Obs - \overline{Obs})}{\sqrt{\sum_1^N (Model - \overline{Model})^2 \sum_1^N (Obs - \overline{Obs})^2}} \quad (A6)$$

623
 624 **Acknowledgement.** This research was supported under Assistance Agreement No.
 625 RD835871 by the U.S. Environmental Protection Agency to Yale University through
 626 the SEARCH (Solutions for Energy, AiR, Climate, and Health) project that supported
 627 L.R. Leung, Y. Zhang, and K. Wang, and by grants from the National Key Project of



628 MOST (2017YFC0209801), National Natural Science Foundation of China (41705124)
629 and the Fundamental Research Funds for the Central Universities that supported J.
630 Zhang, Y. Gao, K. Luo, and J. Fan. It has not been formally reviewed by EPA. The
631 views expressed in this document are solely those of The SEARCH Center and do not
632 necessarily reflect those of the Agency. EPA does not endorse any products or
633 commercial services mentioned in this publication. PNNL is operated for DOE by
634 Battelle Memorial Institute under contract DE-AC05-76RL01830. We thank
635 Khairunnisa Yahya, a former graduate student of the Air Quality Forecasting
636 Laboratory at NCSU for conducting the WRF/Chem simulations used in this work. We
637 acknowledge the World Climate Research Programme's Working Group on Coupled
638 Modelling, which is responsible for CMIP, and we thank the climate modeling groups
639 for producing and making available their model output. Analysis data used to generate
640 the plots in this manuscript can be accessed by contacting Yang Gao
641 (yanggao@ouc.edu.cn), and the WRF/Chem model output can be accessed by
642 contacting Yang Zhang (yzhang9@ncsu.edu).

643

644 **References**

645

- 646 Agrawal, M., B. Singh, M. Rajput, F. Marshall and J. N. B. Bell (2003). Effect of air
647 pollution on peri-urban agriculture: a case study. *Environ. Pollut.* 126(3): 323-329.
- 648 Arora, V., J. Scinocca, G. Boer, J. Christian, K. Denman, G. Flato, V. Kharin, W. Lee
649 and W. Merryfield (2011). Carbon emission limits required to satisfy future
650 representative concentration pathways of greenhouse gases. *Geophys. Res. Lett.*
651 38(5): 387-404.
- 652 Bi, D., M. Dix, S. J. Marsland, S. O'Farrell, H. Rashid, P. Uotila, A. Hirst, E. Kowalczyk,
653 M. Golebiewski and A. Sullivan (2013). The ACCESS coupled model: description,
654 control climate and evaluation. *Aust. Meteorol. Oceanogr. J.* 63(1): 41-64.
- 655 Diffenbaugh, N. S. and F. Giorgi (2012). Climate change hotspots in the CMIP5 global
656 climate model ensemble. *Climatic Change* 114(3-4): 813-822.
- 657 Dix, M., P. Vohralik, D. Bi, H. Rashid, S. Marsland, S. O'Farrell, P. Uotila, T. Hirst, E.
658 Kowalczyk and A. Sullivan (2013). The ACCESS coupled model: documentation
659 of core CMIP5 simulations and initial results. *Aust. Meteorol. Oceanogr. J.* 63(1):
660 83-99.



- 661 Donner, L. J., B. L. Wyman, R. S. Hemler, L. W. Horowitz, Y. Ming, M. Zhao, J.-C.
662 Golaz, P. Ginoux, S.-J. Lin and M. D. Schwarzkopf (2011). The dynamical core,
663 physical parameterizations, and basic simulation characteristics of the atmospheric
664 component AM3 of the GFDL global coupled model CM3. *J. Climate* 24(13): 3484-
665 3519.
- 666 Dufresne, J.-L., M.-A. Foujols, S. Denvil, A. Caubel, O. Marti, O. Aumont, Y.
667 Balkanski, S. Bekki, H. Bellenger and R. Benshila (2013). Climate change
668 projections using the IPSL-CM5 Earth System Model: from CMIP3 to CMIP5.
669 *Clim. Dynam.* 40(9-10): 2123-2165.
- 670 Filleul, L., S. Cassadou, S. Medina, P. Fabres, A. Lefranc, D. Eilstein, A. Le Tertre, L.
671 Pascal, B. Chardon, M. Blanchard, C. Declercq, J. F. Jusot, H. Prouvost and M.
672 Ledrans (2006). The relation between temperature, ozone, and mortality in nine
673 french cities during the heat wave of 2003. *Environ. Health Persp.* 114(9): 1344-
674 1347.
- 675 Fiore, A. M., V. Naik and E. M. Leibensperger (2015). Air Quality and Climate
676 Connections. *J. Air Waste Manage.* 65(6): 645-685.
- 677 Flynn, J., B. Lefer, B. Rappengluck, M. Leuchner, R. Perna, J. Dibb, L. Ziemba, C.
678 Anderson, J. Stutz, W. Brune, X. R. Ren, J. Q. Mao, W. Luke, J. Olson, G. Chen
679 and J. Crawford (2010). Impact of clouds and aerosols on ozone production in
680 Southeast Texas. *Atmos. Environ.* 44(33): 4126-4133.
- 681 Gantt, B., J. He, X. Zhang, Y. Zhang and A. Nenes (2014). Incorporation of advanced
682 aerosol activation treatments into CESM/CAM5: model evaluation and impacts on
683 aerosol indirect effects. *Atmos. Chem. Phys.* 14(14): 7485-7497.
- 684 Gao, Y., J. S. Fu, J. B. Drake, J. F. Lamarque and Y. Liu (2013). The impact of emission
685 and climate change on ozone in the United States under representative concentration
686 pathways (RCPs). *Atmos. Chem. Phys.* 13(18): 9607-9621.
- 687 Gao, Y., J. S. Fu, J. B. Drake, Y. Liu and J. F. Lamarque (2012). Projected changes of
688 extreme weather events in the eastern United States based on a high resolution
689 climate modeling system. *Environ. Res. Lett.* 7(4): 044025.
- 690 Gao, Y., L. R. Leung, J. Lu, Y. Liu, M. Y. Huang and Y. Qian (2014). Robust spring
691 drying in the southwestern U. S. and seasonal migration of wet/dry patterns in a
692 warmer climate. *Geophys. Res. Lett.* 41(5): 1745-1751.
- 693 Glotfelty, T., J. He and Y. Zhang (2017). Impact of future climate policy scenarios on
694 air quality and aerosol-cloud interactions using an advanced version of
695 CESM/CAM5: Part I. model evaluation for the current decadal simulations. *Atmos.*
696 *Environ.* 152: 222-239.
- 697 Glotfelty, T. and Y. Zhang (2016). Impact of future climate policy scenarios on air
698 quality and aerosol-cloud interactions using an advanced version of CESM/CAM5:
699 Part II. Future trend analysis and impacts of projected anthropogenic emissions.
700 *Atmos. Environ.* 152: 531-552.
- 701 Gryparis, A., B. Forsberg, K. Katsouyanni, A. Analitis, G. Touloumi, J. Schwartz, E.
702 Samoli, S. Medina, H. R. Anderson, E. M. Niciu, H. E. Wichmann, B. Kriz, M.



- 703 Kosnik, J. Skorkovsky, J. M. Vonk and Z. Dortbudak (2004). Acute effects of ozone
704 on mortality from the "Air pollution and health: A European approach" project. *Am.*
705 *J. Resp. Crit. Care.* 170(10): 1080-1087.
- 706 Guenther, A., T. Karl, P. Harley, C. Wiedinmyer, P. I. Palmer and C. Geron (2006).
707 Estimates of global terrestrial isoprene emissions using MEGAN (Model of
708 Emissions of Gases and Aerosols from Nature). *Atmos. Chem. Phys.* 6: 3181-3210.
- 709 He, J. and Y. Zhang (2014). Improvement and further development in CESM/CAM5:
710 gas-phase chemistry and inorganic aerosol treatments. *Atmos. Chem. Phys.* 14(17):
711 9171-9200.
- 712 Horton, D. E., C. B. Skinner, D. Singh and N. S. Diffenbaugh (2014). Occurrence and
713 persistence of future atmospheric stagnation events. *Nat. Clim. Change* 4(8): 698-
714 703.
- 715 Hou, P. and S. L. Wu (2016). Long-term Changes in Extreme Air Pollution Meteorology
716 and the Implications for Air Quality. *Sci. Rep.* 6: 23792.
- 717 Jacob, D. J. and D. A. Winner (2009). Effect of climate change on air quality. *Atmos.*
718 *Environ.* 43(1): 51-63.
- 719 Jones, C., J. Hughes, N. Bellouin, S. Hardiman, G. Jones, J. Knight, S. Liddicoat, F.
720 O'Connor, R. J. Andres and C. Bell (2011). The HadGEM2-ES implementation of
721 CMIP5 centennial simulations. *Geosci. Model. Dev.* 4(3): 543.
- 722 Kharin, V. V., F. W. Zwiers, X. Zhang and M. Wehner (2013). Changes in temperature
723 and precipitation extremes in the CMIP5 ensemble. *Climatic Change* 119(2): 345-
724 357.
- 725 Leonard, M., S. Westra, A. Phatak, M. Lambert, B. van den Hurk, K. McInnes, J. Risbey,
726 S. Schuster, D. Jakob and M. Stafford-Smith (2014). A compound event framework
727 for understanding extreme impacts. *Wiley Interdisciplinary Reviews: Climate*
728 *Change* 5(1): 113-128.
- 729 Leung, L. R. and W. I. Gustafson (2005). Potential regional climate change and
730 implications to US air quality. *Geophys. Res. Lett.* 32(16): 367-384.
- 731 Meehl, G. A. and C. Tebaldi (2004). More intense, more frequent, and longer lasting
732 heat waves in the 21st century. *Science* 305(5686): 994.
- 733 Mesinger, F., G. Dimego, E. Kalnay, P. Shafran, W. Ebisuzaki, D. Jovic, K. Mitchell, H.
734 Berbery, Y. Fan and W. Higgins (2005). North American Regional Reanalysis:
735 Evaluation Highlights and Early Usage. *Bull. Amer. Meteor. Soc.* 87(3): 561-608.
- 736 Moss, R. H., J. A. Edmonds, K. A. Hibbard, M. R. Manning, S. K. Rose, D. P. van
737 Vuuren, T. R. Carter, S. Emori, M. Kainuma, T. Kram, G. A. Meehl, J. F. B. Mitchell,
738 N. Nakicenovic, K. Riahi, S. J. Smith, R. J. Stouffer, A. M. Thomson, J. P. Weyant
739 and T. J. Wilbanks (2010). The next generation of scenarios for climate change
740 research and assessment. *Nature* 463(7282): 747-756.
- 741 Otero, N., J. Sillmann, J. L. Schnell, H. W. Rust and T. Butler (2016). Synoptic and
742 meteorological drivers of extreme ozone concentrations over Europe. *Environ. Res.*
743 *Lett.* 11(2): 24005.
- 744 Qian, Y., S. J. Ghan and L. R. Leung (2010). Downscaling hydroclimatic changes over



- 745 the Western US based on CAM subgrid scheme and WRF regional climate
746 simulations. *Int. J. Climatol.* 30(5): 675-693.
- 747 Rotstayn, L. D., M. A. Collier, M. R. Dix, Y. Feng, H. B. Gordon, S. P. O'Farrell, I. N.
748 Smith and J. Syktus (2010). Improved simulation of Australian climate and
749 ENSO - related rainfall variability in a global climate model with an interactive
750 aerosol treatment. *Int. J. Climatol.* 30(7): 1067-1088.
- 751 Sarwar, G. and P. V. Bhave (2007). Modeling the effect of chlorine emissions on ozone
752 levels over the eastern United States. *J. Appl. Meteorol. Clim.* 46(7): 1009-1019.
- 753 Scoccimarro, E., S. Gualdi, A. Bellucci, A. Sanna, P. Giuseppe Fogli, E. Manzini, M.
754 Vichi, P. Oddo and A. Navarra (2011). Effects of tropical cyclones on ocean heat
755 transport in a high-resolution coupled general circulation model. *J. Climate* 24(16):
756 4368-4384.
- 757 Seager, R., M. F. Ting, C. H. Li, N. Naik, B. Cook, J. Nakamura and H. B. Liu (2013).
758 Projections of declining surface-water availability for the southwestern United
759 States. *Nat. Clim. Change* 3(5): 482-486.
- 760 Seneviratne, S. I., N. Nicholls, D. Easterling, C. M. Goodess, S. Kanae, J. Kossin, Y.
761 Luo, J. Marengo, K. McInnes and M. Rahimi (2012). Changes in climate extremes
762 and their impacts on the natural physical environment In: *Managing the Risks of*
763 *Extreme Events and Disasters to Advance Climate Change Adaptation* [Field et al.
764 (eds.)]. A Special Report of Working Groups I and II of the Intergovernmental Panel
765 on Climate Change (IPCC). Cambridge University Press, Cambridge, UK, and New
766 York, NY, USA, pp. 109-230.
- 767 Sharma, S., P. Sharma and M. Khare (2017). Photo-chemical transport modelling of
768 tropospheric ozone: A review. *Atmos. Environ.* 159: 34-54.
- 769 Sillmann, J., V. V. Kharin, F. W. Zwiers, X. Zhang and D. Bronaugh (2013). Climate
770 extremes indices in the CMIP5 multimodel ensemble: Part 2. Future climate
771 projections. *J. Geophys. Res-Atmos.* 118(6): 2473-2493.
- 772 Souri, A. H., Y. S. Choi, X. S. Li, A. Kotsakis and X. Jiang (2016). A 15-year
773 climatology of wind pattern impacts on surface ozone in Houston, Texas. *Atmos.*
774 *Res.* 174: 124-134.
- 775 Taylor, K. E., R. J. Stouffer and G. A. Meehl (2012). An Overview of Cmp5 and the
776 Experiment Design. *B. Am. Meteorol. Soc.* 93(4): 485-498.
- 777 Tebaldi, C., J. M. Arblaster and R. Knutti (2011). Mapping model agreement on future
778 climate projections. *Geophys. Res. Lett.* 38: L23701.
- 779 USEPA (2007). *Guidance on the Use of Models and Other Analyses for Demonstrating*
780 *Attainment of Air Quality Goals for Ozone, PM2.5. and Regional Haze.* EPA-
781 454/B-07e002.
- 782 van Vuuren, D. P., J. Edmonds, M. Kainuma, K. Riahi, A. Thomson, K. Hibbard, G. C.
783 Hurtt, T. Kram, V. Krey, J. F. Lamarque, T. Masui, M. Meinshausen, N. Nakicenovic,
784 S. J. Smith and S. K. Rose (2011). The representative concentration pathways: an
785 overview. *Climatic Change* 109(1-2): 5-31.
- 786 Volodin, E., N. Dianskii and A. Gusev (2010). Simulating present-day climate with the



- 787 INMCM4.0 coupled model of the atmospheric and oceanic general circulations. *Izv.*
788 *Atmos. Ocean Phy+* 46(4): 414-431.
- 789 Watanabe, M., T. Suzuki, R. O'ishi, Y. Komuro, S. Watanabe, S. Emori, T. Takemura,
790 M. Chikira, T. Ogura and M. Sekiguchi (2010). Improved climate simulation by
791 MIROC5: mean states, variability, and climate sensitivity. *J. Climate* 23(23): 6312-
792 6335.
- 793 Weare, B. C., C. Cagnazzo, P. G. Fogli, E. Manzini and A. Navarra (2012). Madden -
794 Julian Oscillation in a climate model with a well - resolved stratosphere. *J.*
795 *Geophys. Res-Atoms.* 117(D1): -.
- 796 Weschler, C. J. (2006). Ozone's impact on public health: Contributions from indoor
797 exposures to ozone and products of ozone-initiated chemistry. *Environ. Health*
798 *Persp.* 114(10): 1489-1496.
- 799 Xin, X., T. Wu and J. Zhang (2012). Introductions to the CMIP5 simulations conducted
800 by the BCC climate system model. *Adv. Climate Change Res.* 8: 378-382.
- 801 Yahya, K., P. Campbell and Y. Zhang (2017a). Decadal application of WRF/chem for
802 regional air quality and climate modeling over the US under the representative
803 concentration pathways scenarios. Part 2: Current vs. future simulations. *Atmos.*
804 *Environ.* 152: 584-604.
- 805 Yahya, K., K. Wang, P. Campbell, Y. Chen, T. Glotfelty, J. He, M. Pirhalla and Y. Zhang
806 (2017b). Decadal application of WRF/Chem for regional air quality and climate
807 modeling over the US under the representative concentration pathways scenarios.
808 Part 1: Model evaluation and impact of downscaling. *Atmos. Environ.* 152: 562-
809 583.
- 810 Yahya, K., K. Wang, P. Campbell, T. Glotfelty, J. He and Y. Zhang (2016). Decadal
811 evaluation of regional climate, air quality, and their interactions over the continental
812 US and their interactions using WRF/Chem version 3.6.1. *Geosci. Model. Dev.* 9(2):
813 671-695.
- 814 Yarwood, G., S. Rao, M. Yocke and G. Whitten (2005). Updates to the carbon bond
815 chemical mechanism: CB05 final report to the US EPA. RT-0400675: 2841-2842.
- 816 Yukimoto, S., Y. Adachi, M. Hosaka, T. Sakami, H. Yoshimura, M. Hirabara, T. Y.
817 Tanaka, E. Shindo, H. Tsujino and M. Deushi (2012). A new global climate model
818 of the Meteorological Research Institute: MRI-CGCM3—model description and
819 basic performance—. *J. Meteorol. Soc. Jpn.* 90: 23-64.
- 820 Zanchettin, D., A. Rubino, D. Matei, O. Bothe and J. Jungclaus (2013). Multidecadal-
821 to-centennial SST variability in the MPI-ESM simulation ensemble for the last
822 millennium. *Clim. Dynam.* 40(5-6): 1301-1318.
- 823 Zscheischler, J., A. M. Michalak, C. Schwalm, M. D. Mahecha, D. N. Huntzinger, M.
824 Reichstein, G. Berthier, P. Ciais, R. B. Cook, B. El-Masri, M. Y. Huang, A. Ito, A.
825 Jain, A. King, H. M. Lei, C. Q. Lu, J. F. Mao, S. S. Peng, B. Poulter, D. Ricciuto,
826 X. Y. Shi, B. Tao, H. Q. Tian, N. Viovy, W. L. Wang, Y. X. Wei, J. Yang and N. Zeng
827 (2014). Impact of large-scale climate extremes on biospheric carbon fluxes: An
828 intercomparison based on MsTMIP data. *Global Biogeochem. Cy.* 28(6): 585-600.



829 Zscheischler, J. and S. I. Seneviratne (2017). Dependence of drivers affects risks
830 associated with compound events. *Sci. Adv.* 3(6): e1700263.
831